Fundamentals and Application of Electrowetting on Dielectrics

Francesco Liberale, Roberto Bernasconi and Luca Magagnin*

Dip. Chimica, Materiali e Ing. Chimica Giulio Natta, Politecnico di Milano, Via Mancinelli 7, 20131 Milano, Italy

Received: November 20, 2014 Revised: December 22, 2014 Accepted: January 21, 2015

1. INTRODUCTION

In the last few decades electrowetting, a phenomenon observed for the first time at the beginning of 20th century, has attracted increasing attention due to the possibility of applications in the electronic field. In particular the uses in flexible displays and multifocal lenses have been addressed as the most promising. This article presents the state of the art about these two key application areas together with a brief overview of some advanced applications of electrowetting in fluid manipulation at micrometric scale for lab-on-chip devices. A general review about electrowetting as physical phenomenon is provided as well. Some experimental results are presented in the final part to contextualize the information provided with laboratory data.

2. PHYSICAL PRINCIPLES AND STATE OF THE ART

2.1. Contact Angle and Surface Energy

The presence of an electric field in proximity of a conductor and a dielectric produces a gathering of electrical charges at the interface between the two. The electric field itself then couples with the interfacial electric charges to exert an interfacial force, which, if the interface is deformable (e.g. liquid-gas one), can distort it [1]. The term "electrowetting" indicates a change in the contact angle between a drop of conductive liquid and the surface on which it lies by means of electrostatic charges [2] and, more generally, a variation of the electric forces along the interfacial triple contact lines [1]. To better explain the phenomenon is useful to recall the thermodynamic principles of the interactions at solid-liquid-gas interfaces.

*Address correspondence to this author at the Dip. Chimica, Materiali e Ing. Chimica Giulio Natta, Politecnico di Milano, *Via* Mancinelli 7, 20131 Milano, Italy; Tel: +39 0223993124; Fax: +39 0223993180;
E-mail: luca.magagnin@polimi.it

Generally speaking, a molecule inside a drop is attracted by the adjacent molecules in all the directions with the same intensity, in such a way that the resulting force exerted on it is zero. On the contrary, as depicted in Fig. (**1**), a molecule placed on the surface of the drop experiences just a force in the direction of the inner molecules, being attracted only by these molecules [3, 4]. This attractive force generates the so-called "surface tension", that is the evidence of intermolecular forces at a surface/interfacial level, which is defined as the energy needed to increase the surface area by a unit [5]:

$$\gamma = dW/dA \quad (1)$$

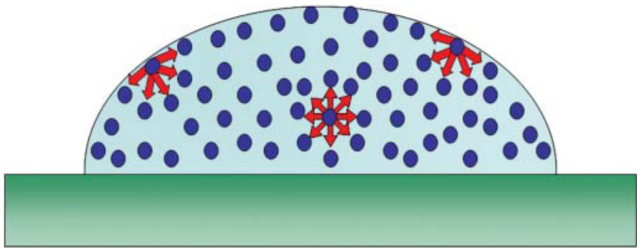

Fig. (1). Molecules on the surface are not equally attracted in all directions; this is the origin of the surface tension. *Reprinted with permission from [4].*

where γ is the surface tension, measured as force per unit length or, equivalently, as energy per unit area, dW is the variation in energy and dA the change in surface area. Being the sphere the geometric form with the smallest surface area at a fixed volume, it is also the configuration with the smallest surface energy, and this explains why a freestanding drop spontaneously assumes a spherical shape [4]. Moreover, volume forces like gravity are usually negligible in the case of small drops.

The surface tension at the interface of two materials depends on their mutual properties and not only on those of one of the two; this statement is confirmed by simple examples from everyday's life: a drop of oil placed on a hydrophobic surface, such that of a Teflon® coated pan, will assume a "less spherical shape" compared with that of a water drop on the same surface, and this is due to the higher permanent dipole moment of water molecules and to their strong intermolecular hydrogen bonds. The surface tension between water and air is about 72 $mJ \cdot m^{-2}$, almost double than that between oil and air [4]. A typical example is mercury, the only liquid metal at room temperature, which has strong inner attractive forces and whose surface tension reaches 485 $mJ \cdot m^{-2}$. The breakage of the old clinical thermometers used to cause in fact the leakage of the metal in the shape of droplets.

At the beginning of the nineteenth century, the English scientist Thomas Young studied the forces at the interfaces of the three phases (substrate, liquid, air), placing some drops on a surface and measuring the so-called contact angle resulting from these measurements. "Contact angle" means the angle formed between the external surface of the drop and the surface on which it lies: a balance of the interfacial forces led to the formulation of the well-known Young equation:

$$\gamma_{LG}\cos\theta + \gamma_{SL} = \gamma_{SG} \quad (2)$$

where γ_{LG} represents the interfacial tension between liquid and gas, γ_{SL} the one between liquid and substrate and γ_{SG} the one between the latter and the gas. A schematic picture of the forces acting at the triple contact line is shown in Fig. (**2**).

The analysis of the contact angle between a drop of water and a substrate allows to determine if the latter is hydrophobic or hydrophilic (the discrimination between the two states is usually set at values of contact angle below or above 90°, while we speak of super hydrophobicity for values greater than 150°). As already mentioned, the values of θ can vary by changing the liquid the drop is made of, the substrate and its morphological features and the fluid of the third phase. Generally, if the polarizability of the material used as a substrate is bigger than the polarizability of the liquid, we have a "complete wetting" of the base material, otherwise only a "partial wetting" of the surface is attained [4].

2.2. Electrowetting

About seventy years after Young's study, the Sorbonne University professor and future Nobel Price Gabriel Lippmann observed a change in the capillary rise of mercury due to the presence of electrical charges and proposed the hypothesis of electrocapillarity, eventually confirmed by experimental tests [4, 6, 7]. A term due to electrical polarization was added to the Young equation (2), generating thus what is now known as the Young-Lippmann equation:

$$\gamma_{LG}\cos\theta + \gamma_{SL} = \gamma_{SG} + \tfrac{1}{2} CV^2 \quad (3)$$

where V is the voltage and C the capacitance per unit area in the region of contact between the metallic surface on which the electrolyte drop lies and the drop itself. The usual experimental setup implies the creation of an electric field applying a potential difference between an auxiliary electrode (for example a needle placed inside the drop) and the metallic surface of the base [8]. The application of the voltage causes the separation of positive and negative charges inside the drop and the force which acts on the same charges inside the liquid produces an increase in the contact area between the drop and the base surface, thus decreasing the contact angle θ. Applying a voltage between the metal of the substrate and the electrolyte drop can give rise to electrochemical reactions, which over time cause irreversible changes at the interface between metal and electrolyte, as for example metal oxidation and electrolyte contamination. This produces a significant decrease in electrowetting events, thus providing results that are useless for application [4].

In the 30's of the last century, Frumkin referred to the electrocapillarity and electrowetting principle to study the behavior of an electrolyte at the interface between a polarized metallic surface and air [6, 9], but more than 50 years had to pass before a revival of interest in these phenomena occurred, with the research and the development of new promising applications. In the late 80s and in the following years, the idea of adding a thin layer of insulating material between the metallic surface and the drop of conductive material became established, thus avoiding or at least limiting the development of electrochemical reactions. This method is called EICE (Electrowetting on Insulator Coated Electrodes) [6] or, more frequently, EWOD (Electrowetting On Dielectric) [2, 4, 8]. A pictorial representation of the EWOD phenomenon is provided in Fig. (**3**).

This method allows observing the phenomenon for numerous cycles of voltage application, providing an optimal stability in time. The equation (3) can be rewritten to make explicit the electrical permittivity in vacuum and in the dielectric (ε_0, ε_r), the thickness of the dielectric (δ), the initial contact angle (θ_0) and the angle with electrowetting (θ_1).

$$\cos\theta_1 = \cos\theta_0 + (\varepsilon_0\varepsilon_r V^2)/(2\delta\gamma_{LG}) \quad (4)$$

The dielectric constant of the medium and the thickness of the insulating layer are the parameters which determine the capacitance per unit area of the surface of contact between the base and the drop. The current research aims at finding insulating materials with high dielectric constant and applicable in low thickness (often few to hundreds of micrometers [6]) and with acceptable costs. The dielectric hydrophobicity is another essential characteristic to have high contact angles at zero voltage and to allow broad θ variations when in use [4]. The presence of a macroscopic insulating film changes the order of magnitude of the voltage V necessary to significantly modify the contact angle. In fact:

$$V \approx \sqrt{\frac{\gamma}{c}} \approx \sqrt{\frac{\delta_\gamma}{\varepsilon_0\varepsilon_r}} \quad (5)$$

Therefore, instead of few tens of millivolts necessary to obtain electrowetting on the metal, tens or hundreds of volts will be needed in the presence of an intermediate insulating layer [6]. Obviously, the maximum voltage limit applied has to be lower than that which would cause the dielectric breakdown. A challenge in the modern EWOD is the need of lowering as much as possible the voltage required to manipulate the droplets [8], in order to make electrowetting potentially competitive and compatible with the current electronic de-

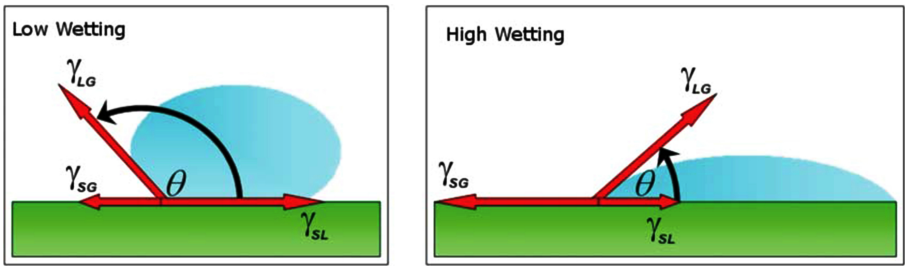

Fig. (2). High inner contact angle and low wetting on the left and low inner contact angle and high wetting on the right. *Reprinted with permission from [4].*

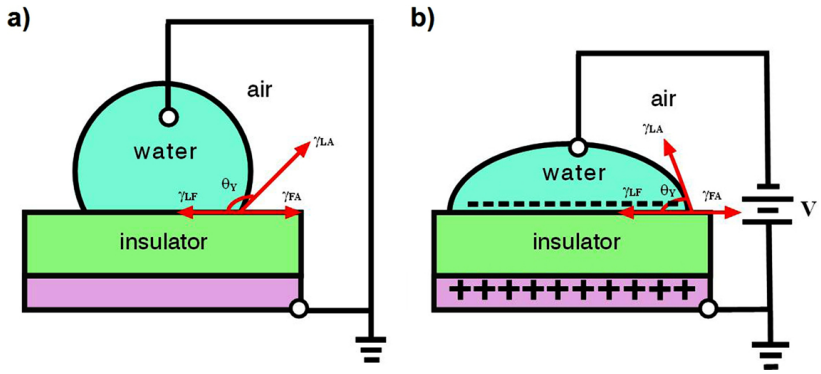

Fig. (3). Configuration with the dielectric, both with zero voltage (Young equation) and with the application of the voltage (Young-Lippmann). *Reprinted with permission from [5].*

vices. Lots of actual devices which operate at low voltage (less than 30V) require deposition techniques which are slow and expensive (ALD or CVD) [10, 11].

An excessive reduction in the dielectric thickness often generates an annihilation of the dielectric properties, with negative consequences such as high electric fields, local defects and uncontrolled oxidation [8]. It has been recently demonstrated that the passivation of the substrate metal allows a control and a self-healing of the existing defects [8, 11-13]. At Cincinnati University [5] it has been proved that the use of surfactants succeeded in reducing γ_{LG}, leading to a reduction of the operative voltage needed to produce electrowetting. In [8] the authors demonstrated the realization of an efficient method to produce substantial contact angle variations with voltages lower than 10V by applying a polymer through spin coating on an aluminum base. In the same article it is reported that the application of an alternate-polarity voltage induces a fast degradation of the aluminum surface after just a few cycles because of the high cathodic reaction speed, while a positive voltage produces a negligible degradation.

The Young-Lippmann equation can be derived by adopting different approaches. The most widely used and accepted are the thermodynamic method, the energy minimization method and the electromechanical method [1, 14]. Despite the theoretical validity of the equation and its experimental validation in a wide variety of devices and applications, some aspects of electrowetting are still not completely justified [4]. The most evident phenomenon is without doubt the contact angle saturation obtained by applying high voltages, a theoretically not justified event [1, 4, 5, 14] and for which some physical and mathematical methods are suggested to give an interpretation [15, 16]. In [17] the authors experimentally demonstrate that using DC voltage, the contact angle saturation is invariant with the electric field, the contact line's profile, the interfacial tension, the choice of insulating non-polar fluids and the kind of conductive polar fluids. Moreover, saturation occurs in different ways and at different angles in AC or DC experiments [6]. Another not completely understandable aspect concerns the hysteresis between repeated ON and OFF states of the voltage [1, 4, 6, 14], a circumstance which is unacceptable or at least constrictive due to the low reproducibility. A reduction of this phenomenon happens when adding salts inside the water which forms the drops, providing thus a source of ions to allow the free movement of charges in the liquid [4, 17]. Finally, when the voltage (AC) applied is frequency dependent and we are in the 10-100 KHz frequency range or above, the water drops behave no more as ionic conductors but as dielectrics [4]. As previously observed in Fig. (**3**), a generic EWOD system can be schematized as a parallel plate capacitor; despite this general statement, peculiar phenomena are experimentally observed due to the electrical chargesgathering in the drop in proximity to the interface with the other two phases, as it usually happens in every conductor for the edge effect [6]. This charge accumulation causes repulsion between adjacent drops, which will not tend to coalesce. Another experimental evidence with the same origin is represented by the expulsion of small droplets from the main drop at high voltages, a phenomenon which is attenuated when some salt is added in the drop solution [6].

2.3. Applications

The possibility of moving a liquid without aid of mechanical equipments, but simply by applying a voltage and

obtaining response times on the order of milliseconds, makes electrowetting a potential candidate for the development of new and affordable applications in a great deal of research fields. The number of scientific publications on this topic has indeed considerably increased in the last twenty years, also thanks to the possibility of designing and producing efficient devices on the micro and nanoscale. The main applications include the use in "lab-on-chip" devices [1, 14, 18, 19], in biomedical and chemical equipment in which reliability of transport and manipulation of micrometric drops is essential [20-25], in the development of optical systems (lenses) with variable focal length [4, 26-29] and in the production of electronic displays [4, 5, 14, 29-33].

We now briefly present the manufacture of lenses with variable focal length and, more in detail, the research on displays (even on flexible substrate), always taking advantage of the electrowetting phenomenon.

2.3.1. Variable Focal Length Lenses

Up to a few years ago, all optical devices used a system of lenses mutually moving to focus on images at different distances. This implied the use of a mechanical apparatus, with limitations in the durability, miniaturization and impact resistance of the device. Recently, innovative devices have been developed [26-29] and commercialized. They allow varying the lenses focal length simply by modifying the reciprocal curvature of water and oil droplets placed in a cell thanks to the application of electrical charges, as schematically shown in Fig (**4**). The voltage application is indeed proportional to the fluid curvature and allows to finely set the focalization of objects at different distances. This technique not only permits a miniaturization of the device while maintaining a very good reliability, but it also minimizes the risk of breakage or malfunctioning of the optical apparatus.

2.3.2. Electrowetting Displays

In the last few years another field which profited from intensive research and application of electrowetting is that of electronic display manufacture. Currently, the market is dominated by backlit transmissive displays based on LCD technology. However, this presents some limitations such as high energy consumption, high weight, rigidity and not optimal readability in intense lighting conditions; moreover, transmission efficiency is less than 10% [5]. Recently, reflective displays for e-paper applications have been produced exploiting different technologies: electrophoretic, electrochromic, cholesteric liquid crystals, micro-electromechanical interference, liquid powders and electrowetting [33]. Electrowetting itself has the most promising features for large-scale production and commercialization [34]. Electrowetting possesses a mix of characteristics which make it a potentially wide-diffusion technology in the near future: excellent visibility from all angles, even with intense sunlight, rapid response speed (order of milliseconds), high clearness and color brilliance, and compatibility with the actual LCD production techniques [5].

Before describing the electrowetting displays working principle, we recall the basic rudiments of the nowadays available displays: the emissive, transmissive and reflective types [5]. The emissive displays are known for their large viewing angle and ability of working in a wide temperature range. Notwithstanding, these factors are coupled with some disadvantages such as a reduction of contrast and readability when the ambient is abundantly illuminated and the necessity of using color filters. The transmissive displays need a backlight to illuminate a front panel, thus offering optimal contrast to the display and brilliant images. On the other side, energy consumption is high and readability inadequate in conditions of high outdoor illumination. Finally, reflective displays use reflected ambient light to create images: this causes low energetic consumption, low weight and optimal visibility with intense sunlight. A "hybrid" display proposed modality [5] is the "transreflective" one, which can produce transmissive, reflective images or a combination of the two as required. Displays based on electrowetting (EWD) can operate in a versatile way in the three modalities, reflective,

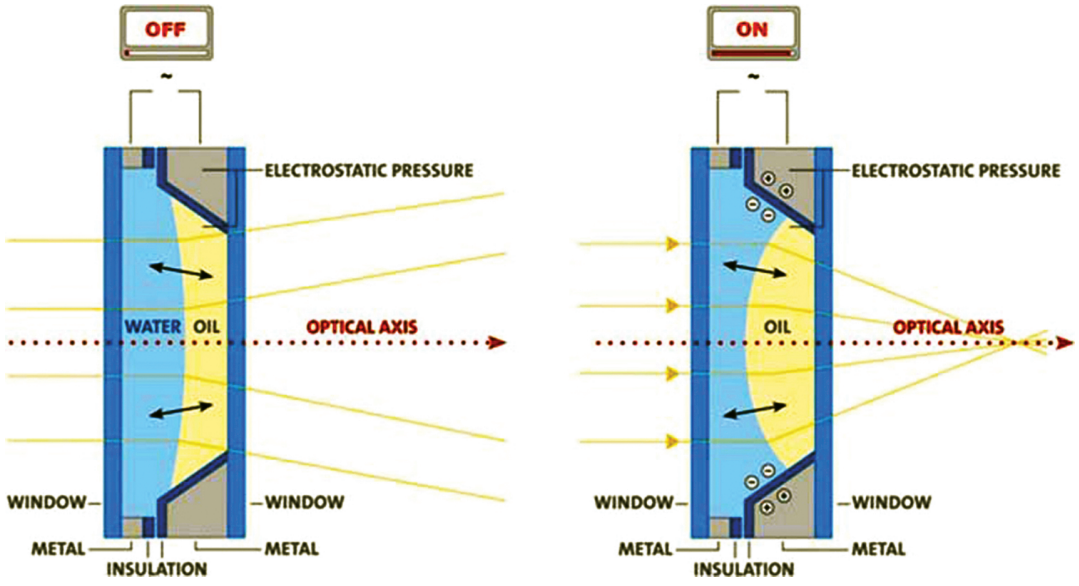

Fig. (4). Section of a lens without voltage application (left): it can be observed that light, passing from water to oil, is diffused by the latter. After voltage application, fluid curvature changes and oil convexity permits to focus light on a point (right). *Reprinted with permission from [4].*

transmissive and emissive one [30-32]. Electrowetting allows to create a "valve" for light by moving two immiscible liquids, one transparent and one colored, by means of the application of an electric field [13, 14, 30-32], as shown in Fig. (**5**).

As presented in Fig. (**5**), the pixel structure is formed by a substrate (glass or polymer), an electrode, a hydrophobic dielectric, hydrophilic grids, colored oil, deionized water and a top glass with ITO (not shown in the figure). In equilibrium conditions, without voltage application, the oil layer completely wets the bottom of the cell to minimize the energetic balance because the surface tension between oil and insulator is lower than that between the latter and water. When applying a voltage, the free charges in the water are attracted by the electrode and water itself "pushes" oil towards the cell edges, thus opening the "valve" and letting light pass through [4, 5]. The micrometric dimensions which can be currently obtained in the pixel production let the surface tension forces dominate over the gravity ones, allowing the use of the device in every spatial configuration. The speed of transition between the ON and OFF state is determined by the liquid viscosity and by the friction of the drop with the underlying surface and is in the order of milliseconds, thus permitting the video reproducibility with this technique [4]. From the general principle of the monochromatic cell described above, it is easy to pass to the structure of a colored pixel [4, 30-32]. Actually, two different configurations exist. The first, as depicted in Fig. (**6**), implies the lateral connection of a trio of cells, each one containing one of the three primary colors, and the modulation of each color to obtain the desired resulting color. The resolution is satisfactory, even if reduced by a third compared with that offered by a monochromatic pixel.

A second configuration considers instead the creation of a single chromatic unit with three layers containing colored oil with cyan, magenta and yellow colors overlapped. The cell structure is built as in Fig. (**7**) and exhibits two overlapping units: the lower one contains two oil layers, one in magenta color on the top and one in cyan color on the bottom; the upper one contains the yellow oil. The final color of each pixel is modulated by controlling the surface area occupied by each oil layer through electrowetting. No decrease in the resolution is observed with respect to the monochromatic case, because the pixel dimension is the same in the two configurations [4, 30-32].

Lao, in his dissertation [5], describes in detail the materials and methods adopted in the production of electrowetting pixels. In particular, he compares the standard manufacturing process of pixels for the transmissive modality with an inno-

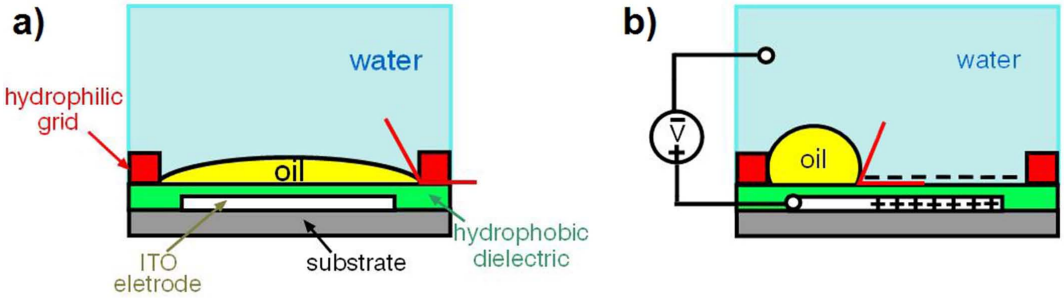

Fig. (5). OFF and ON state of the pixel. *Reprinted with permission from [5].*

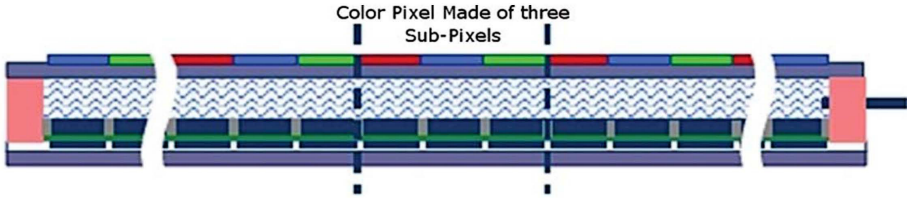

Fig. (6). Colored Pixel formed by three laterally flanked units. *Reprinted with permission from [4].*

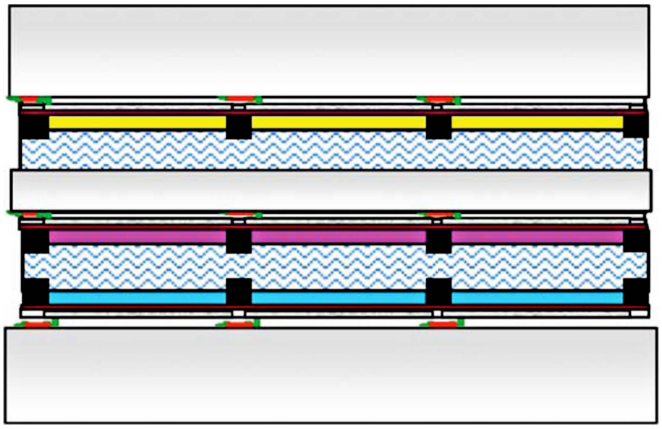

Fig. (7). Colored pixel formed by overlapping layers containing oil in different colors. *Reprinted with permission from [4].*

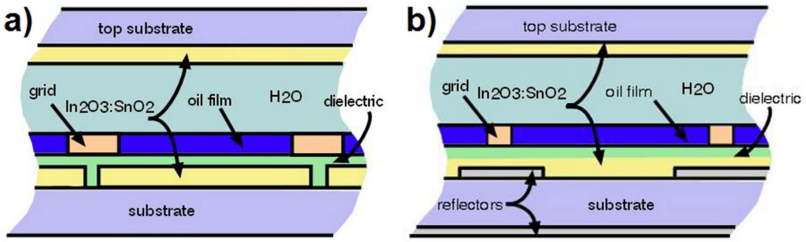

Fig. (8). Standard EWD and reflector-enhanced EWD. *Reprinted with permission from [5].*

vative method to increase efficiency by inserting some metal reflectors in the device. Below is a short report on the process used and the results obtained. As it can be observed in Fig. (**8**), the structure of a standard EWD (shown in Fig. **5**) and that of an EWD with reflectors only differentiate for the presence of reflectors (Al) between the substrate and the inferior electrode.

The manufacture consists of the following steps, as showed in Fig. (**9**): a) the base is a substrate, usually made of glass; b) a thin aluminum layer is applied on the glass base through sputtering and the desired reflectors profile is obtained with a lithographic technique, c) an ITO layer or another type of electrode is deposited again through sputtering: unavoidable electrode feature is transparency; d) coating with hydrophobic dielectric follows, which, remembering equation (4), must have high dielectric constant and reduced thickness. Numerous candidates were used in the experiments, among which "ParyleneC" had unsatisfactory performances for thicknesses lower than one micron, and solid inorganic dielectrics such as SiN, SiO_2 and Al_2O_3 did not presents sufficiently high hydrophobicity, which, on the contrary, is a typical quality of the Cytop fluoropolymer. Three configurations have been chosen to obtain the dielectric layer: 1) Parylene C and Fluoropel, 2) SiN and Fluoropel, 3) SiN and Cytop; e) the patterning of the hydrophilic grids with a lithographic technique followed, with the aim of creating "walls" for the single pixels; f) finally, the colored oil dosage.

In order to reduce the interfacial tension between oil and water and consequently the voltage to apply to obtain electrowetting, surfactants can be used, as proposed by [5]. Experimental tests showed that a dielectric thickness reduction produces an increase in the contact angle change for the same voltage applied. Moreover, with the use of surfactants, the voltage required to obtain the same oil movement is reduced by a half. It has also been demonstrated that the use of a dielectric multilayer made of SiN and Fluoropel has a dielectric constant (and so also a capacitance per unit area) higher than that of a multilayer made of Parylene C and Fluoropel and it allows to obtain the same contact angle changes results by applying lower voltages. Since no sufficiently low operating voltages were obtained in the first two configurations (lower than 15V), SiN combined with Cytop has been used as hydrophobic multilayer with satisfactory results.

Despite the abundant advantages offered by electrowetting, some improvements are still needed to obtain an optimal competitiveness of this technology in the manufacture of displays. The main challenge concerns the optical contrast between the ON and OFF states of the pixel when miniaturizing the system more and more. In fact a dimensional reduction also implies a reduction in the oil layer thickness, and by doing this oil can become partially transmissive. The biggest efforts in this field are made in the search for colorants with improved optical absorbance [5]. Another issue concerns the transition speed to the initial state, once voltage is removed. During this passage, oil goes back thanks to the lower interfacial tension with the substrate; in this time interval a reduction in the process speed is observed when oil approaches the total pixel coverage and this is due to the fact that, being oil near the equilibrium, it is submitted to a lower driving force. In [5] the author suggests the use of reflectors inside the cell to minimize the time for this passage and so bring it below 10 ms. The need to deposit these reflectors leads to prefer solid dielectrics like SiN/SiO_2 instead of the organic ones for their better resistance to high temperatures in the production steps [5]. Always in reference [5], in order to reduce the display energetic costs, instead of applying a constant voltage, the use of a higher initial transitory is suggested, and then a lower voltage than the usual one. To obtain this, the type of hydrophobic layer used has to be optimized to avoid the charge entrapment during the initial pulse phase and also the geometry of the transparent electrode has to be improved.

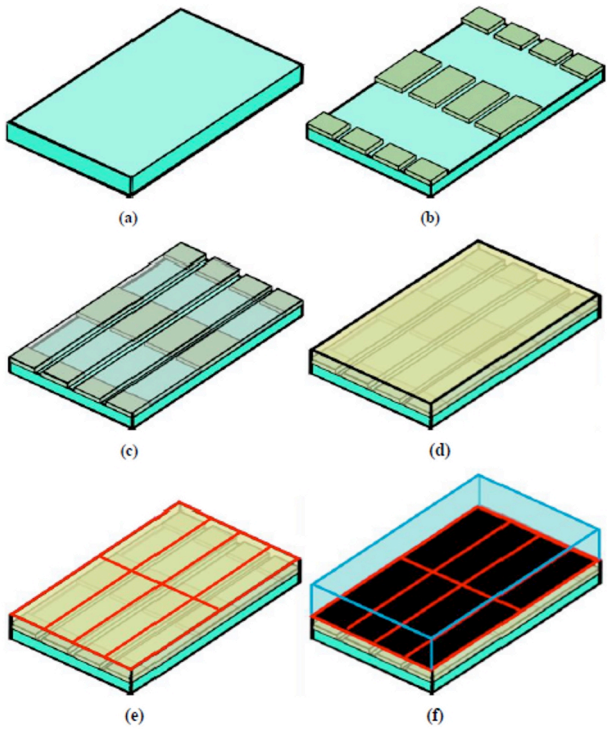

Fig. (9). Manufacturing steps of reflector-enhanced EWD. *Reprinted with permission from [5].*

Furthermore, in [33] authors underline that 20% of a pixel area is always occupied by colored oil even during voltage application, that the colorant does not yield the same performance of solid pigments in terms of color and durability and that the system is not "bistable", which means it needs continuous voltage application to maintain oil pushed towards the edges. They have suggested to build a 3D structure to increase contrast and to use pigmented colorants instead of the usual ones. The proposed structure is shown in Fig. (**10**). The principal components include a reservoir for the liquid pigments which does not occupy more than 10% of the visible area, a channel system for pigment diffusion and spreading in the ON state until 80-95% coating is reached and finally a lateral duct to allow the passage of non-polar liquid once the reservoir is empty. In this way, in the quiescent state the pigment occupies a limited portion of the pixel, staying confined inside the cavity; applying instead the voltage between liquid and one electrode, the electromechanical pressure exceeds the Young-Laplace pressure and the fluid is forced to pass in the microchannels. Decreasing the reservoir area to 5% of the pixel, a contrast ratio of 20:1 is obtained.

2.3.3. Electrowetting on Flexible Substrates

In these years the research on non-planar or flexible electronic systems is getting great impulse and it can be foreseen that the use of flexible displays will be soon extensively diffused in a great number of applications, such as paper-like displays for reading of books or newspapers, play or packaging displays, or those used in the biomedical field [31]. Electrowetting represents a promising technique in this direction since it is not limited by the monochromaticity and by the operative slowness of the electroforetic displays or by the rigidity of the most widely diffused LCD displays. At the Cincinnati University [30-32] it has been demonstrated that the contact angle change can happen on flexible substrates made of different materials with performances not so far from those on the traditional glass base. In particular, electrowetting experiments have been performed on paper, polymeric and metallic substrates, all with a certain curvature. Fig. (**11**) shows an electrowetting diagram on a curved paper base. The above structure is made of a paper base on which a transparent conductor, e.g. ITO, or a reflecting metal, e.g. copper, are deposited to form the electrode; then the deposition of the dielectric and, finally, of the fluoropolymer follows. Over this last layer (not shown in the figure), a flexible hydrophilic grid is created with a lithographic process to confine oil, all sealed with a PDMS top covering. Alternatively to paper, polymeric PET or flexible copper and steel substrates have been used, as depicted in Fig. (**12**). The results of contact angle changes as a function of the applied voltage follow the theoretical predictions up to a voltage of 55 V, lower than both the saturation limit and the dielectric breakdown. Deviations from the foreseen behavior are ascribable to the charges entrapment in the dielectric and to its surface quality.

Besides, the completely correct working of the device in the transition between the ON and OFF states, both in a curved configuration and during bending, has been evidenced. This circumstance has also been proved by the creation of the already mentioned and more complex electrofluidic 3D structure [33], in which the authors underline that the possibility of keeping process temperatures below 120° translates into a perfect compatibility with polymeric substrates. Moreover, a broad temperature range (-28° to 80°C) is admitted, thanks to the stability of the pigment dispersion in the polar fluid. In [31] considerable contact angle changes (between 30° and 40°) have been reported on flexible substrates made of paper, copper and aluminum. Smaller variations have been observed with steel sheets instead, perhaps

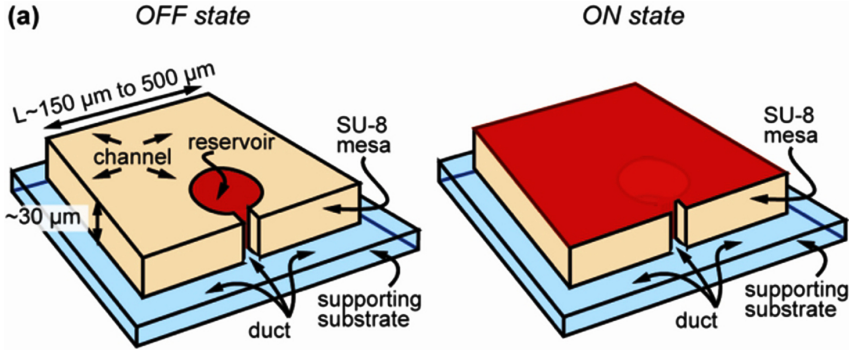

Fig. (10). Schematic representation of an electrofluidic cell. *Reprinted with permission from [33].*

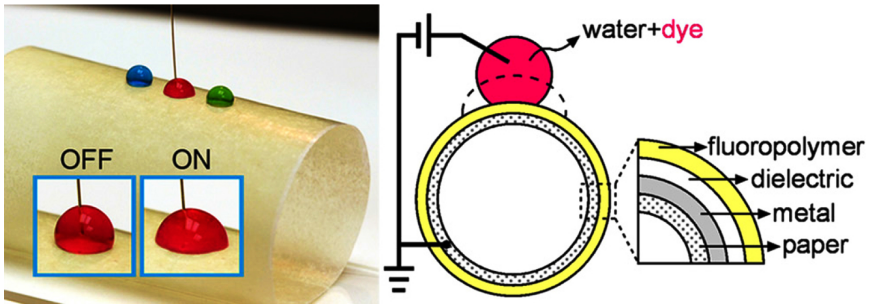

Fig. (11). Electrowetting diagram on curved paper base. *Reprinted with permission from [30].*

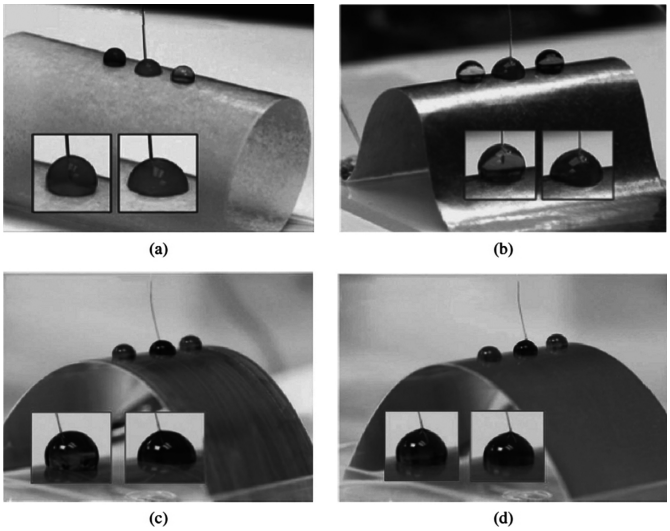

Fig. (12). Electrowetting on different flexible substrates: **a**) paper covered with ITO, **b**) paper covered with copper, **c**) thin copper sheet on steel sheet, **d**) steel sheet. *Reprinted with permission from [31].*

due to the presence of a residual oxide layer not removed from its surface. The increase in the dielectric thickness causes the contact angle variation to diminish at the same voltage applied. If the wetting times for metal surfaces are comparable with those for paper, the wetting times for the inverse process, passing from an ON to an OFF state, are greater for metal surfaces because of their higher roughness.

2.3.4. Microfluidic Applications

An important and promising application of the electrowetting phenomenon concerns the production of microdevices for the control of the position and the motion of drops of fluid. We speak of "digital microfluidics" (DMF) and with this term is indicated the emission of drops from a reservoir, their movement from an electrode to the next one, the mixing with other drops to combine different chemical and biological species to obtain the desired reaction and the division in smaller droplets [14, 35]. All these processes can be obtained applying electrical potentials to a series of electrodes on which the drops lie [14]: these microelectrodes are usually embedded in a solid substrate covered with an hydrophobic layer, each one having approximately the dimensions of a drop and are positioned to form a grid which allow the activation of a single and precise position inside the grid itself [35]. The advantages offered by the "digital microfluidic" are many and comprise the possibility of manipulating small volumes of liquid with optimal accuracy, diminishing thus the amount of reagents used, increasing at the same time the throughput of the process and reducing significantly the operative times [2, 35]. Most of the nowadays existing microfluidic systems try to pursue these aims through the use of systems made of pumps, channels and valves, choices which all imply a quite high energy demand for the functioning and which do not guarantee an optimal efficiency because of gas bubbles formation at the channel's junctions. Moreover, the actual microfluidic systems do not take advantage of a dominating force at the microscopic level, surface tension [2]. Nowadays two different kinds of microsystems which exploit the electrowetting to manipulate the drops exist: "open" systems, in which the drop freely lies on a horizontal substrate and "covered" systems, in which the drop is comprised between two plates. Each of the two configurations has its advantages and disadvantages [2, 35]; dispensing, movement and division of drops is simpler in the "covered" configuration, while merging, mixing and evaporation are favored by the "open" one. We now briefly report the differences which manifest in the process of division, dispensing, merging and mixing of drops, as presented by [35].

The process of drop division implies the presence of a hydrophobic zone embedded between two hydrophilic ones: in these two a force of elongation is created in opposite directions, thus producing a pinching in the central part, as shown in Fig. (**13**).

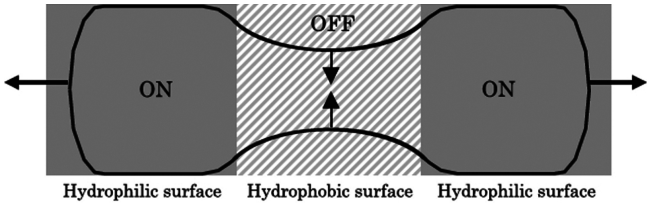

Fig. (13). Stretching force applied in the lateral sides, combined with a pinching force in the center. *Reprinted with permission from [1].*

For an open system, both the numerical simulations and the experimental data show the impossibility of dividing the drops through electrowetting because the forces generated are not enough to elongate the drop and cause a division. The only way to divide the drops in an open system is that of elongating in advance the drops with respect to the application of the electrowetting voltage. Ionic liquids have a better behavior thanks to their elasticity and to the lower contact angle they form with the underlying surface. The possibility of dividing the drop in a closed system is higher than in the previous case, provided that the vertical aperture between the two surfaces has a value below a certain threshold.

The emission of drops from a reservoir proceeds following some steps and can't be performed in all the conditions. Both the numerical simulation and the experimental results show how the fluid dispending in an open system is impossible for aqueous solutions or buffering biological solutions. In a closed system the dispensing is made up of three phases, controlled modulating the potential difference between the device's electrodes and the drop: a) and b) outcome of the liquid from the reservoir; c) pinching of the liquid extrusion; d) separation by back pumping. The process is exemplified in Fig. (**14**).

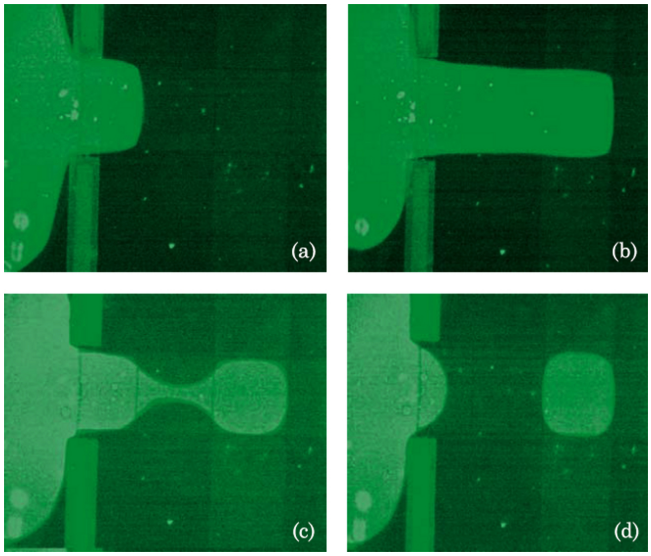

Fig. (14). a) and **b**) liquid extrusion from the reservoir, **c**) pinching of the liquid extrusion, **d**) separation by back pumping. *Reprinted with permission from [1].*

It has been moreover proved that the surface tension has little influence on the possibility or modality of drops emission. The electrodes shape has a not irrelevant influence for what concerns the emission of drops from a reservoir: as the drops are dispensed, the volume of liquid in the reservoir diminishes and is thus necessary to maintain with accuracy the position of the remaining liquid. Two different configurations for the electrodes have been proposed, the "spike-shaped" one and the "star-shaped" one: the first guarantees the centering of the drop in front of the opening gate, the second the creation of zero resultant electro-capillary forces when the droplet is positioned at the center of the electrode itself.

Despite being intuitively a simple phenomenon, the mixing of two drops is a complex physical process. In the laminar state mixing is promoted by diffusion and by stretching and folding of the streamlines. Mixing of liquids in open systems is quite simple as long as the viscosity of the fluid is low: in this case the Marangoni effect is the dominant feature. For liquids with higher viscosity, like ionic liquids, this effect seems ineffective and the mixing efficiency is very low. The liquid behaves like "gels". Mixing fluids in closed systems is more complicated. There are mainly three different processes, all with the aim of increasing the striation process: 1) back and forth motion, 2) successive division and merging operations and 3) loop motions [35]. Another relevant feature which can be handled with electrowetting is the dilution of solutes, always presented in [35]. Dilution of reactants is a very important operation in chemistry and even more in biology: with traditional methods, that is by using pipettes, the control on the diluted concentrations cannot be extremely high. EWOD can be well adapted to precise dilution operations. Obviously the dilution of discrete entities, like particles, magnetic beads, cells and so on still remains a phenomenon of complex handling. These are indeed subjected to body forces like gravity, interaction forces and Brownian motion and their homogenization in the liquid is quite difficult, even with electrowetting.

2.4. The Role of Metal Oxide in a EWOD System

As already observed and expressed in equation (3), the most direct methods to minimize the applied voltage during electrowetting in the presence of a dielectric (EWOD) are a thinner insulating layer and/or a material with high dielectric constant. Both these methods contain some criticalities: the first would indeed cause an increase of the electric field inside the dielectric itself, thus increasing the risk of breakdown; the second opens the way to the use of new and promising dielectric materials, whose integration with the current devices, however, is not free from uncertainties. As already mentioned, the presence of a polymeric layer (usually a fluoropolymer) above the base electrode is essential to test high initial contact angles (θ_0) and wide variations of the same angle during service. Great importance is also assumed by the configuration and morphology of the metallic oxide which is formed on the base electrode, in the case this is actually made of metal. In [36] the authors study the dielectric properties of the oxide electrochemically grown on the base metal, leaving out the further application of the polymeric layer. The anodization of different metals leads to the creation of oxides with high dielectric constants: Al_2O_3(ε_r=9), Ta_2O_5(ε_r=22), ZrO_2 and HfO_2 (ε_r=25). Despite having the lowest dielectric constant among the listed oxides, the choice of studying the behavior of aluminum oxide was done, since aluminum anodization is well known and extensively used. The kind of oxide formed depends mainly on the nature of the electrolyte used: the more neutral its pH, the more compact the oxide, while a higher acidity of the solution generates a more porous oxide. During the anodization process the oxide film grows for migration of metallic ions and oxygen anions in opposite directions, that is at the interface between metal and oxide and between oxide and electrolyte. The final oxide thickness, measurable with the use of an ellipsometer, is proportional to the anodization voltage used at constant times. The dielectric film degradation, observable through an increase of electrical conductivity inside the layer itself when a high defect density is reached, can be caused by phenomena happening both at the solid-dielectric interface and inside the oxide itself. The loss in performance of the dielectric film is studied in two different configurations: the first, completely at the solid state, is made up by a metal-oxide-metal junction, the second by electrolyte-oxide-metal junction. The dielectric breakdown in the first configuration is imputable to the activation of defect states (creation and emission of electrical charges) in different voltage ranges, like Shottky and Poole-Frenkel emissions and Fowler-Nordheim tunnel-

ing. Applying opposite bias, different dielectric breakdown values and asymmetric I-V characteristics are obtained because of inhomogeneous charges distribution in the growing oxide. In the second configuration, an even more pronounced asymmetry at opposite bias is observed. With cathodic polarization hydrogen absorption and evolution take place, which imply a reduction and dissolution of oxide at low voltages; with anodic polarization, oxide growth restarts once the anodization voltage is overcome and the dielectric breakdown is not observed until hydrogen evolution occurs when the voltage is increased.

In [37] the authors give evidence that the application of a thermal treatment in argon atmosphere between 200° and 400°C can reduce electrical conductivity in the oxide following an increase of the energetic barrier needed for the emission of the charges contained in the same. With cathodic polarization, the defectiveness should be brought down to values below 10^{17} cm^{-3}, enough to not observe a gas evolution and to have a current reduction of three orders of magnitude. Under anodic polarization, the defectiveness decrease delays the start of ionic conduction and limits a further growth as well as a breakdown of oxide.

2.5. Pending Questions

Generally speaking electrowetting is a complex phenomenon, constituted by the combination of different physical aspects which can act on different dimensional scales, depending on the kind of application selected: this versatility let us understand from one side the applicative potentialities of electrowetting, from the other side the existing difficulties for an accurate handling of different phenomena, often at microscale level. Nowadays broad ranges to improve the commercial offer of devices exploiting the electrowetting phenomenon still exist. Great opportunities for the research and the subsequent application will be certainly offered by studies on the electrowetting dynamics, especially on the micro and nanometric scale and with flexible substrates. Since the leading research on electrowetting is oriented toward the displays production, a great interest is represented by the study of phenomena related to small drops, even through their interaction with instrumentations like AFM, SEM and TEM microscopes [14]. Moreover more and more precise and affordable modeling of the drops interfacial dynamics will be needed to support the experimental results or to predict the behavior in complex fluidodynamic situations.

3. EXPERIMENTAL METHODS

The aluminum used in the experiments is a laminate with a thickness of about 200 μm and purity higher than 99%. For the anodization a 2% wt. boric acid solution brought to a pH value of 7 through the addition of ammonium hydroxide was used [38-41]. All chemicals were purchased by Sigma Aldrich and used as received. The experimental setup was made up of a 250ml becker containing the solution, two small aluminum plates to be used as cathode and anode respectively and of a potentiostat-galvanostat Amel 7050 to provide the anodization potentials and to register the current transients during the anodization itself. The natural oxide existing on the Al layer, whose thickness is about 5nm [42], was not removed. The aluminum plates were degreased with acetone, washed in deionized water and dried with a nitrogen flux. A voltage range between 10 and 40 V was selected for anodizing the samples, increasing the voltage between each single test of 10 V. The anodization time was fixed at 40 minutes for each sample and the solution was slightly agitated with a magnetic stirrer during the process, always at room temperature. At the end of each anodization every sample was washed with deionized water and dried with a nitrogen flux. Then the contact angle formed between a water drop and the aluminum oxide surface was measured. To perform this test a camera placed in front of a backlit panel was used in order to collect the images of the drops supplied by a syringe on the anodized samples. The camera was coupled with the program "Drop Shape Analysis" to save and elaborate the data obtained. For each sample three zones were considered to acquire the values of contact angle, and mean values are reported; a standard deviation of about 5% was observed for contact angle measurements. For SEM analysis, a Zeiss Evo 50 EP equipped with an EDS module Oxford Inca Energy 200 EDS was used. For the electrowetting tests, a 0.6% solution of AF 1600 fluoropolymer from Dupont in FC40 solvent from 3M was employed. In particular the samples have been immersed for 5 seconds inside a beaker containing the solution and then dried in air. After 30 minutes a second immersion was performed, and after other 30 minutes an annealing at 200°C in air for 1 hour in a Salvislabvacu center. The thickness of the polymer was estimated using an interferometer Filmetrics F20. Using a potentiostat EA-PSI 8360-IST it was possible to supply electrical charges to the drops coming out from the syringe by means of the needle.

4. RESULTS

In this section some experimental results obtained in our laboratory are shown: they aim at testing the efficiency of the anodized aluminum as a substrate, even a flexible one, on which electrowetting can be attained. The ease in processing aluminum in thin sheets combined with its good flexibility allows to consider this material as a candidate for electrowetting applications.

4.1. Anodization

The purpose of the first tests was to obtain, through oxidation, a compact and continuous oxide layer. Strongly acidic electrolyte solutions like hydrofluoric and oxalic acid ones were therefore excluded and among those weakly acidic or neutral a 2% wt. boric acid solution in water was chosen [38-41]. The variables in the process are many and concern not only the choice of the solution and its pH but also the material selection for the cathode, the relative distance between anode and cathode, the voltage applied with the generator and the process time. Only some of them were changed during the experimentation, in an effort to provide a first characterization of the process. In Fig. (**15**) are shown the graphs of the mean contact angle values obtained on the aluminum before the anodization (0V) and after anodization at 10, 20, 30, 40 V and the relative current transient data collected in the first anodization intervals.

Initial contact angle on native aluminum oxide is significantly high but consistent with previous measurements done

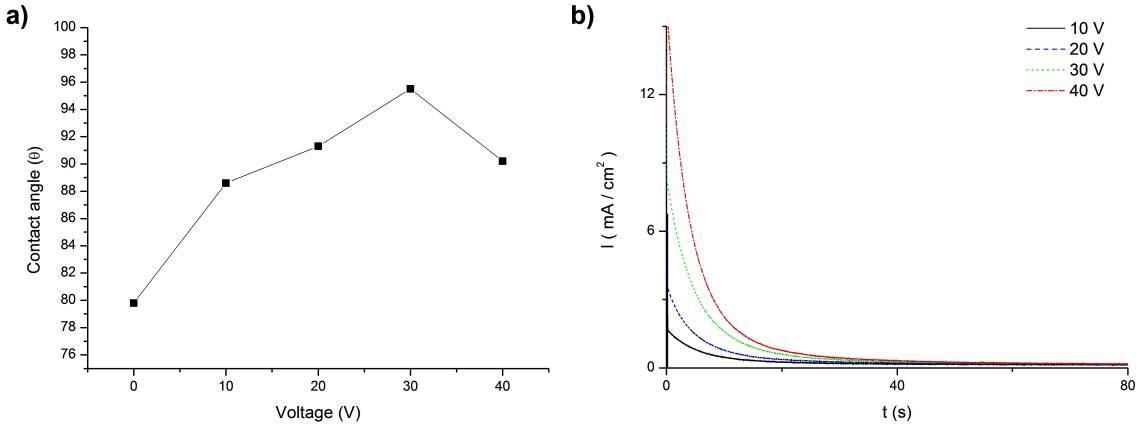

Fig. (15). Contact angles observed on non anodized and anodized Al (**a**); current transient for the anodization process (**b**).

using sessile drop fitting [43, 44]. Such high contact angle was attributed in the past to organic surface contamination [43] as a consequence of polishing processes. However, the native Al was cleaned deeply using acetone, and no polishing was performed. In the case of the anodized samples, the solution used in the present work does not include any organic component. It is therefore possible that the high contact angle is correlated to the presence of impurities in the Al substrate, as possibly evidenced by the EDS. It can be noticed that the contact angle is higher than reference values reported in the literature [45] for sulfate/oxalate electrolytes. Such processes produce nanoporous Al_2O_3 characterized by a honeycomb structure, while the treatment described in the present work provide compact layers with nanometric roughness. As can be noticed from Fig. (**15 a**) a progressive enhancement of the contact angle increasing the anodization voltage up to 30 V is observed, while it slightly decreases with an anodization voltage of 40 V, fact probably ascribable to partial oxide damage at these voltages. The change in contact angle with respect to the anodization voltage is reasonably justified by the different surface morphology obtained in correlation to the thickness of the Al_2O_3 layer. The graph (**15 b**) shows how the anodization currents asymptotically tend to values near to zero increasing the process times. In particular, at the end of the anodization, after 40 minutes, current density values of about 0.1 mA/cm^2 are registered. Moreover, higher initial currents were observed when increasing the anodization potential. The thickness of the oxide layer after anodization reported in literature ranged between 20 and 50 nm [37].

4.2. Characterization

To characterize the anodized samples, scanning electron microscope SEM and energy dispersive X-rays spectroscopy analyses were performed. From the latter, observing the peaks intensities, the substantial presence of the oxygen peak is noticed, as reported in Fig. (**16b**). The two peaks at 2 and 3 eV are related to the gold layer applied by sputtering on the oxide to make possible the SEM observation. The existence of a compact oxide without porosity has been then confirmed from the observation of the samples surface, as shown in Fig. (**16a**). Furthermore, EDS data exclude the possibility of organic contamination of the surface and of the oxide layer.

4.3. Electrowetting

The application of the polymer on the anodized samples followed the anodization, with the aim of observing electrowetting. This allowed observing a decrease in the contact angle that the drops formed on the anodized surface once the voltage was applied, that is the evidence of the electrowetting. The thickness of the polymeric layer was estimated to be 1μm, with significant variations along the sample (in the order of ± 0.4μm). The presence of thickness variations on the surface can imply different resulting morphologies, which can justify the different starting values for the contact angle of the samples in Fig. (**17**). In particular some cyclic voltage application tests have been performed, and this allowed to study the trend of the contact angle hysteresis over time; by definition the contact angle hysteresis is defined as the difference between the contact angles at which triple

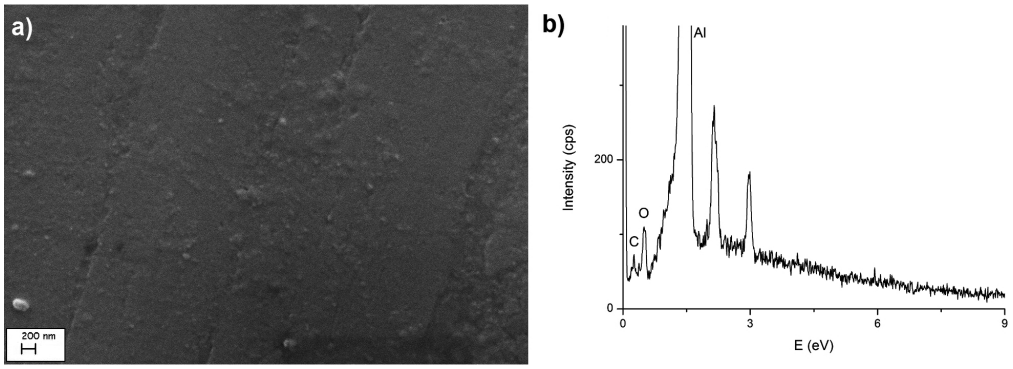

Fig. (16). SEM image of the surface for 20 V anodized sample (a); EDS of the same sample.

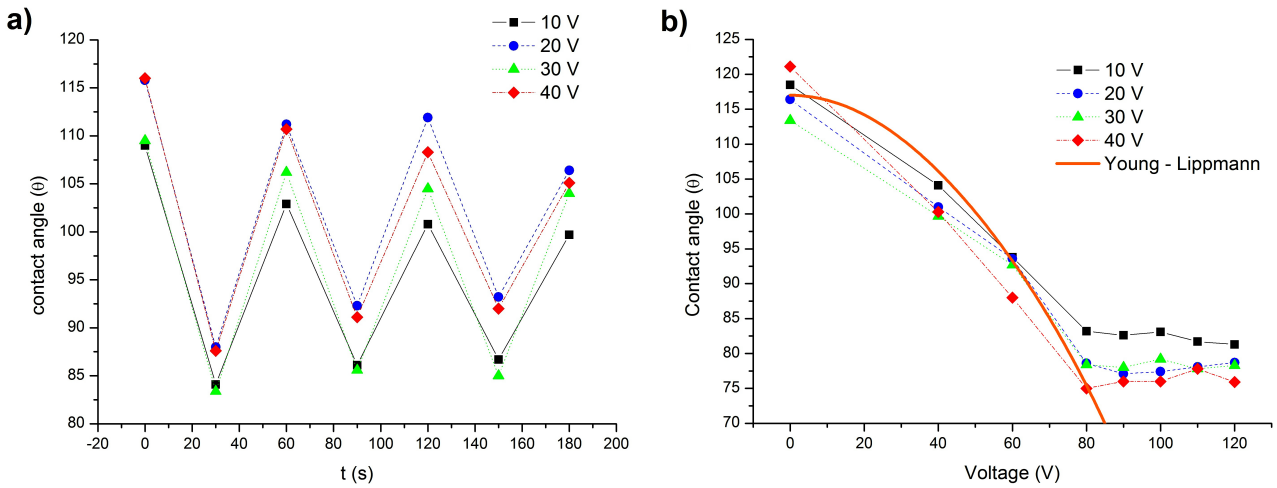

Fig. (17). Hysteresis (**a**) and saturation (**b**) of the contact angle for the samples obtained at different anodization conditions.

contact angle line advances and recedes, known as advancing and receding angles, respectively [46]. In the example shown in Fig. (**17 a**), voltage cycles between 0 V and 60 V have been applied at a distance of 30 seconds one from the other for all the samples, anodized at 10, 20, 30 and 40 V. It can be observed that the difference between the ON and the OFF-state angles is considerably reduced: this phenomenon can be partially ascribed to charges trapping in some points of the device, in particular on the sharp edges of the drop [6] and in the fluoropolymer [47]. Theoretically, when the electrowetting potential is removed, the surface charge should completely dissipate, but as accumulation of trapped charges almost always occurs, asymmetric wetting is observed and in some extreme cases the droplet no longer responds to changes in the applied voltage.

By progressively increasing the applied voltage it was also possible to observe the contact angle saturation for voltages higher than 80 V, as depicted in Fig. (**17b**). For all the samples anodized at different voltages a reduction in the contact angle is observed till a voltage of 80 V. For higher voltage values a significant change in the contact angle is no more evident. This can be related to a damage of the dielectric layer made up of the double polymer coating and by the underlying aluminum oxide or to an effective saturation due to the characteristics of the film. In Fig. (**17b**), the Young-Lippmann relation (equation 4 calculated for the following properties of the polymer: $\varepsilon_r = 2$, $\delta = 1\mu m$) is plotted in comparison with the experimental data, showing an acceptable adherence until the saturation onset.

CONCLUSIONS

Electrowetting represents a phenomenon of great interest. Even though the basic physical principles are known since more than one century, it was only in the last decades that a widespread interest for their application in different promising fields was established. Moreover there are some aspects theoretically still not justified but which clearly manifest experimentally. Only through a better theoretical comprehension of these phenomena their subsequent handling and control, even at the micro and nanoscale, will be possible. Different electrowetting applications are nowadays available on the market, and their diffusion will be more and more widespread in the next years. Among these are variable focal lenses for cameras and optical devices without the need of rigid lenses, low energy consumption displays (even on flexible substrates) and lab-on-chip devices for the accurate movement of biological fluids. We can thus state that electrowetting represents a phenomenon which will acquire more and more attractiveness in the next years, especially because its area of interest is not limited to a pure scientific and laboratory research but it extends to promising commercially available applications. Aluminum is a promising material for electrowetting applications. This statement is confirmed by the experimental results disclosed in the present paper, which represent a starting point for a more articulated research on possible advanced applications of aluminum in the fields presented in the state of the art section. Some issues, nowadays not completely addressed, must be considered: hysteresis, response time of the device and others. These will be subject of future developments.

CONFLICT OF INTEREST

The authors confirm that this article content has no conflict of interest.

ACKNOWLEDGEMENTS

Declared none.

REFERENCES

[1] Berthier, J. *Microdrops and Digital Microfluidics*, 2nd ed.; William Andrew Inc.: Norwich, **2008**.

[2] Cooney, C.G.; Chen, C.Y.; Emerling, M.R.; Nadim, A.; Sterling, J.D. Electrowetting droplet microfluidics on a single planar surface. *Microfluid. Nanofluid.*, **2006**, *2*, 435-446.

[3] Burakowsky, T.; Wierschon, T. *Surface Engineering of metals*, 1st ed.; CRC press: Boca Raton, **1999**.

[4] Shamai, R.; Andelman, D.; Berge, B.; Hayes, R. Water, electricity, and between… On electrowetting and its application. *Soft Matter*, **2008**, *4*, 38-45.

[5] Lao, Y. Ultra-high transmission electrowetting displays. Master thesis, University of Cincinnati: Cincinnati, June **2008**.

[6] Quilliet, C.; Berge, B. Electrowetting: a recent outbreak. *Curr. Opin. Colloid Interface Sci.*, **2001**, *6*, 34-39.

[7] Mugele, F.; Baret, J.C. Electrowetting: from basics to applications. *J. Phys. Condens. Matter*, **2005**, *17*, R705-R774.

[8] Khodayari, M.; Carballo, J.; Crane, N.B. A material system for reliable low voltage anodic electrowetting. *Mater. Lett.*, **2012**, *69*, 96-99.

[9] Froumkine, A. *Couche double, Electrocapillarité, Surtension*; Hermann et C.: Paris, **1936**; pp. 5-36.

[10] Raj, B.; Smith, N.R.; Christy, L.; Dhindsa, M.; Heikenfeld, J. In: *Composite dielectrics and surfactants for low voltage electrowetting devices*, Proceedings of 2008 17th Biennial University/Government/Industry Micro/Nano Symposium, Piscataway, NJ, USA, July13-16, **2008**; pp. 187-90.

[11] Dhindsa, M.; Heikenfeld, J.; Weekamp, W.; Kuiper, S. Electrowetting without Electrolysis on Self-Healing Dielectrics. *Langmuir*, **2011**, *27*, 5665-5670.

[12] Crane, N.B.; Volinsky, A.A.; Mishra, P.; Rajgadkar, A.; Khodayari, M. Bidirectional electrowetting actuation with voltage polarity dependence. *Appl. Phys. Lett.*, **2010**, *96*, 104103.

[13] Nelson, C.W.; Lynch, C.M.; Crane, N.B. Continuous electrowetting *via* electrochemical diodes. *Lab Chip*, **2011**, *11*, 2149-2152.

[14] Zhao, Y.P.; Wang, Y. Fundamentals and Applications of Electrowetting: A Critical Review. *Rev. Adhes. Adhes.*, **2013**, *1*, 114-174.

[15] Klarman, D.; Andelman, D.; Urbakh, M. A Model of Electrowetting, Reversed Electrowetting and Contact Angle Saturation. *Cond-Mat. Soft*, **2011**, 18.

[16] Chevalliot, S.; Kuiper, S.; Heikenfeld, J. Experimental Validation of the Invariance of Electrowetting Contact Angle Saturation. *J. Adhes. Sci. Technol.*, **2011**.

[17] Tan, X.; Zhou, Z.; Cheng, M.M.C. Electrowetting on dielectric experiments using graphene. *Nanotechnology*, **2012**, *23*, 375501.

[18] Pollack, M.G.; Shenderov, A.D.; Fair, R.B. Electrowetting-based actuation of droplets for intergrated microfluidics. *Lab Chip*, **2002**, *2*, 96-101.

[19] Cho, S.K.; Moon, H.; Kim, C.J. Creating, transporting, cutting, and merging liquid droplets by electrowetting-based actuation for digital microfluidic circuits. *J. Microelectromech. Syst.*, **2003**, *12*, 70-80.

[20] Srinivasan, V.; Pamula, V.K.; Fair, R.B. An integrated digital microfluidic lab-on-a-chip for clinical diagnostics on human physiological fluids. *Lab Chip*, **2004**, *4*, 310-315.

[21] Yoon, J.Y.; Garrel, R.L. Preventing biomolecular adsorption in electrowetting based biofluidic chips. *Anal. Chem.*, **2003**, *75*, 5097-5102.

[22] Wheeler, A.R.; Moon, H.; Kim, C.J.; Loo, J.A.; Garrell, R.L. Electrowetting-based microfluidics for analysis of peptides and proteins by matrix-assisted laser desorption/ionization mass spectrometry. *Anal. Chem.*, **2004**, *76*, 4833-4838.

[23] Fair, R.B.; Khlystov, A.; Tailor, T.D.; Ivanov, V.; Evans, R.D.; Griffin, P.B.; Vijay, S.; Pamula, V.K.; Pollack, M.G.; Zhou, J. Chemical and biological applications of digital microfluidic devices. *IEEE Des. Test Comput.*, **2007**, *24*, 10-24.

[24] Karuwan, C.; Sukthang, K.; Wisitsoraat, A.; Phokharatkul, D.; Pattnanasettakul, V.; Wechsatol, W.; Tuantranont, A. Electrochemical detection on electrowetting-on-dielectric digital microfluidic chip. *Talanta*, **2011**, *84*, 1384-1389.

[25] Ratner, D.M.; Murphy, E.R.; Jhunjhunwala, M.; Snyder, D.A.; Jensen, K.F.; Seeberger, P.F. Microreactor-based reaction optimization in organic chemistry—Glycosylation as a challenge. *Chem. Commun.*, **2005**, *5*, 578-580.

[26] Kuiper, S.; Hendriks, B.H.W. Variable-focus liquid lens for miniature cameras. *Appl. Phys. Lett.*, **2004**, *85*, 1128-1130.

[27] Li, C.; Jiang, H. Electrowetting-driven variable-focus microlens on flexible surfaces. *Appl. Phys. Lett.*, **2012**, *100*, 231105.

[28] Berge, B.; Peseux, J. Variable focal lens controlled by an external voltage: an application of electrowetting. *Eur. Phys. J. E*, **2000**, *3*, 159-163.

[29] Simon, E.; Berge, B.; Gaton, H.; Jacques-Sermet, O.; Laune, F.; Legrand, J.; Maillard, M.; Moine, D.; Verplanck, N. Optical Image Stabilization with Liquid Lens; **2010**; http://www.varioptic.com/media/uploads/publication/optical_image_stabilization_odf2010.pdf; last access on 2 October 2014.

[30] Steckl, A.J.; You, H.; Kim, D.Y. In: *Flexible electrowetting and electrowetting on flexible substrates*, Proceedings of SPIE 2011, San Francisco, CA, USA, January 22, **2011**, vol. 7956 795907.

[31] You, H.; Steckl, A.J. Electrowetting on Flexible Substrates. *J. Adhesion Sci. Technol.*, **2011**.

[32] Steckl, A.J.; You, H.; Kim, D.Y. In: *Electrowetting: a flexible electronic-paper technology*, Proceedings of SPIE 2011, San Francisco, CA, USA, February 3, **2011**, vol. 7956 795607.

[33] Zhou, K.; Dean, K.A.; Heikenfeld, J. Flexible Electrofluidic Displays Using Brilliantly Colored Pigments. *SID Symp. Dig. Tech.*, **2010**, 484-486.

[34] www.liquavista.com website, last access 24th October 2014.

[35] Berthier, J. *Microdrops and Digital Microfluidics*, 2nd ed.; William Andrew Inc.: Norwich, **2008**, pp. 225-284.

[36] Mibus, M.; Jensen, C.; Hu, X.; Knopse, C.; Reed, M.L.; Zangari, G. Dielectric breakdown and failure of anodic aluminum oxide for electrowetting systems. *J. Appl. Phys.*, **2013**, *114*, 014901.

[37] Mibus, M.; Jensen, C.; Hu, X.; Knopse, C.; Reed, M.L.; Zangari, G. Improving Dielectric Performance in Anodic Aluminum Oxide *via* Detection and Passivation. *Appl. Phys. Lett.*, **2014**, *104*, 244103.

[38] Harkness, A.C.; Young, L. High resistance anodic oxide film on aluminum. *Can. J. Chem.*, **1966**, *44*, 2409-2413.

[39] Li, Y.; Shimada, H.; Sakairi, M.; Shigyo, K.; Takahashi, H.; Seo, M. Formation and Breakdown of Anodic Oxide Films on Aluminum in Boric Acid/Borate Solutions. *J. Electrochem. Soc.*, **1997**, *144*, 866-876.

[40] Naieff, T.M.; Rashid, K.H. In: *Comparative Study for Anodizing Aluminum Alloy 1060 by Different Types of Electrolytes Solutions*, Proceedings of the first scientific conference on modern technologies in oil and gas refinery, University of technology and midland refineries company, April 25-27, **2011**.

[41] Bertorelle, E. *Trattato di Galvanotecnica*, 1st ed.; Hoepli: Milan, **1977**.

[42] Wafers, K.; Misra, C. *Oxides and Hydroxides of Aluminum*; AlcoaTechnical Report No. 19 Revised, Alcoa Laboratories, **1987**, p. 64.

[43] Bernardin, J.D.; Mudawar, I.; Walsh, C.B.; Franses, E.I. Contact Angle Water Dependence for Water Droplets on Practical Aluminum Surfaces. *Int. J. Heat Mass Transf.*, **1997**, *40*(5), 1017-1033.

[44] Diana, A.; Castillo, M.; Brutin, D.; Steinberg, T. Sessile Drop Wettability in Normal and Reduced Gravity. *Microgravity Sci. Technol.*, **2012**, *24*(3), 195-202.

[45] Redon, R.; Vazquez-Olmos, A.; Mata-Zamora. M.E.; Ordonez-Medrano, A.; Rivera-Torres, F.; Saniger, J.M. Contact Angle Studies on Anodic Porous Alumina. *Rev. Adv. Mater. Sci.,* **2006**, *11*(1), 79-87.

[46] Gupta, R.; Boone, T.; Sheth, D.; Sevilla, A.; Frechette, J. In: *Influence of Contact Angle Hysteresis on Electrowetting Performance*, Proceedings of the 34th Adhesion Society Annual Meeting, Savannah, USA, 13-16 February 2011, The Adhesion Society, **2012**, p. 116.

[47] Berry, S. *Electrowetting Phenomenon for Microsized Fluidic Devices*. PhD Thesis, Tufts University: Medford/Somerville, May **2008**.